

# Privacy-Aware Detection of Fake Identity Documents: Methodology, Benchmark, and Improved Algorithms (FakeIDet2)

Javier Muñoz-Haro, Ruben Tolosana, Julian Fierrez,  
Ruben Vera-Rodriguez, Aythami Morales

*Biometrics and Data Pattern Analytics Lab, Universidad Autónoma de Madrid, Ciudad Universitaria de Cantoblanco, Madrid, 28049, Madrid, Spain*

---

## Abstract

Remote user verification in Internet-based applications is becoming increasingly important nowadays. A popular scenario for it consists of submitting a picture of the user's Identity Document (ID) to a service platform, authenticating its veracity, and then granting access to the requested digital service. An ID is well-suited to verify the identity of an individual, since it is government issued, unique, and nontransferable. However, with recent advances in Artificial Intelligence (AI), attackers can surpass security measures in IDs and create very realistic physical and synthetic fake IDs. Researchers are now trying to develop methods to detect an ever-growing number of these AI-based fakes that are almost indistinguishable from authentic (*bona fide*) IDs. In this counterattack effort, researchers are faced with an important challenge: the difficulty in using real data to train fake ID detectors. This real data scarcity for research and development is originated by the sensitive nature of these documents, which are usually kept private by the ID owners (the users) and the ID holders (e.g., government, police, bank, etc.). The present study proposes a new privacy-aware methodology for research and development in fake ID detection that promotes collaboration between ID holders and AI researchers. In practice, the main contributions of our study are: 1) We present and discuss our proposed patch-based methodology to preserve privacy in fake ID detection research. 2) We provide a new public database, FakeIDet2-db, comprising over 900K real/fake ID patches extracted from 2,000 ID images, acquired using different smartphone sensors, illumination and height conditions, etc. In addition, three physical attacks are considered: print, screen, and composite. 3) We present a new privacy-aware fake ID detection method, FakeIDet2, which introduces two novel learnable modules: Patch Embedding Extractor and Patch Embedding Fusion. 4) We release a standard reproducible benchmark that considers physical and synthetic attacks from popular databases in the literature. The results achieved by our proposed FakeIDet2 in detecting very realistic fake IDs under unseen type of attacks are encouraging: 8.90% and 13.84% Equal Error Rate (EER) in the very challenging datasets DLC-2021 and KID34K, respectively. FakeIDet2-db and the accompanying benchmark are publicly available<sup>1</sup>.

---

<sup>1</sup><https://github.com/BiDALab/FakeIDet2-db>

---

## 1. Introduction

Analyzing the veracity of digital information is one of the great challenges facing society today [2, 37]. With the great advances made in the field of Generative AI, it is possible to synthesize non-existent content or to modify existing content [21, 26, 36], using simple and fast tools easily available on the Internet. These methods can be used for good purposes, for example, correct biases [29] or improve performance in some scenarios where data scarcity is present [22, 32], but they have their downsides, as they can also be used for malicious purposes, such as creating DeepFakes that are harmful [35, 36] or misinformation [18]. Evidence of the latter has been found in recent news, where tampered documents<sup>1</sup> or synthetic<sup>2</sup> were used for the purchase of underage alcohol or to bypass remote verification systems such as Know Your Customer (KYC) to access digital services such as crypto exchanges or digital banking.

In order to advance in this challenging topic, the present study focuses on Presentation Attack Detection (PAD) [12, 16] on Identity Documents (IDs)<sup>3</sup>. Concretely, as can be seen in Fig. 1, we focus on the most popular physical attacks in real-world scenarios: *i) print* attacks are physical fake IDs created using an image or a scanned Identity Document (ID), which is printed on glossy paper to resemble the texture and appearance of real IDs; *ii) screen* attacks, which consist in taking a picture of an ID displayed on a digital screen such as a laptop, tablet, or smartphone; and *iii) composite* attacks, which do not require to tamper an entire document, but only small portions, such as date of birth, family name or the portrait image from the ID owner. In the particular case of *physical composite* attacks, the impostor first prints fields with fake information on colored paper that resembles the colors of the target ID, and then crops each field. After that, these crops are lied on the ID document, occluding the original information with the fake one. All these kinds of attacks, a.k.a. Presentation Attack Instruments (PAIs), are currently being used by attackers to surpass KYC procedures, which explicitly require capturing live images of the user ID using a smartphone camera, granting them access to digital services using fake identities.

Several studies have preliminarily analyzed the problem of fake ID detection, proposing very valuable ideas and resources [5, 7, 15]. However, there are several limitations in the field that need to be covered in a proper way to advance this research direction. First, there are no public databases with official (a.k.a. bona fide) IDs acquired under variable conditions, nor a standard benchmark that evaluates the performance of fake ID detection systems in real-world scenarios. So far, all public databases in the literature consider “real” IDs some created by researchers under laboratory conditions, not official governments. From now on, we refer to these non-official IDs created by research groups as “real” (with quotation marks). As a result, these “real” IDs lack important

---

<sup>1</sup><https://www.nytimes.com/2025/02/13/nyregion/students-high-tech-fake-ids.html>

<sup>2</sup><https://www.404media.co/inside-the-underground-site-where-ai-neural-networks-churn-out-fake-ids-onlyfake/>

<sup>3</sup>Other related works define ID as “Identity”. Here we define ID as “Identity Document”.

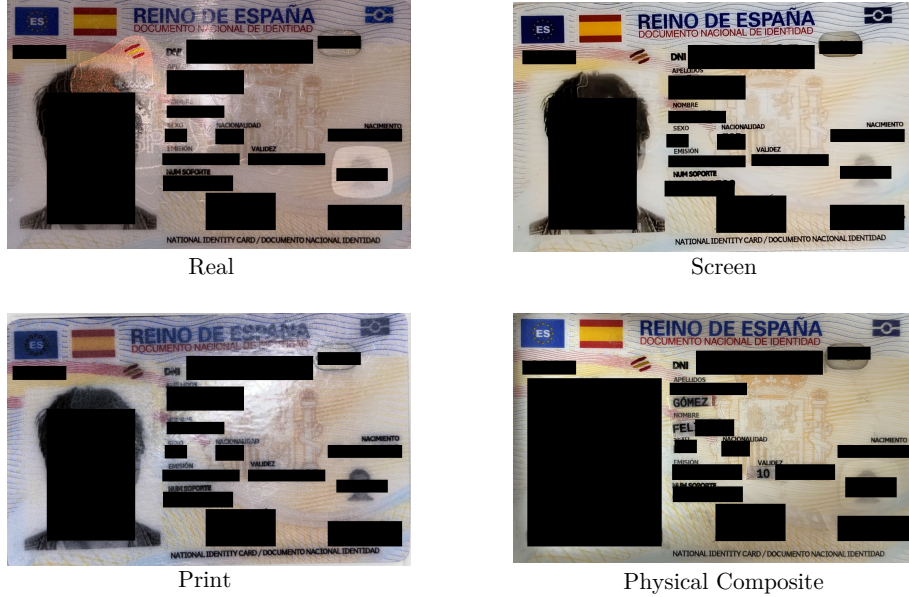


Figure 1: Examples of a real ID and popular physical attacks (print, screen, and physical composite) available in our proposed FakeIDet2-db. The personal information is redacted in this figure to protect the privacy of the subject.

information and patterns such as watermarks, not representing therefore a fidelity scenario of the problem. Some efforts have recently been made in this direction through the organization of international challenges such as DeepID<sup>4</sup> (although the evaluation was private and is not publicly available yet) highlighting a considerable gap in performance between using “real” IDs and the official ones (0.99 vs 0.71 F1 score for the winner of the challenge). The main reason for considering this “real” scenario is due to privacy concerns, as some fields of the IDs contain very sensitive information. These observations from state-of-the-art research trigger our *key motivation for the present study: to research privacy-aware methods where more realistic data than the commonly used “real” data can be used to develop better fake ID detectors based on machine learning, while keeping the data handling as private as possible.*

In the present study, we hypothesize that using *patches* from IDs, instead of the whole ID, to train fake ID detectors might provide benefits from both the performance and privacy points of view in real-world scenarios. Fig. 2 provides a graphical representation of the current scenario considered today for the problem of fake ID detection (top), versus our proposed privacy-aware scenario (bottom). In both scenarios, there are two main actors: *ID Holders* (e.g., government, police, bank, etc.), which provide digital services to citizens and own large-scale datasets of real IDs, and the *AI Researchers* (e.g., research institutions), which have the experience and technology to develop fake ID detectors, but not the data. The current scenario based on sharing the whole ID raises privacy concerns, limiting the development of robust fake ID detectors. Also, there are

<sup>4</sup><https://deepid-iccv.github.io/>

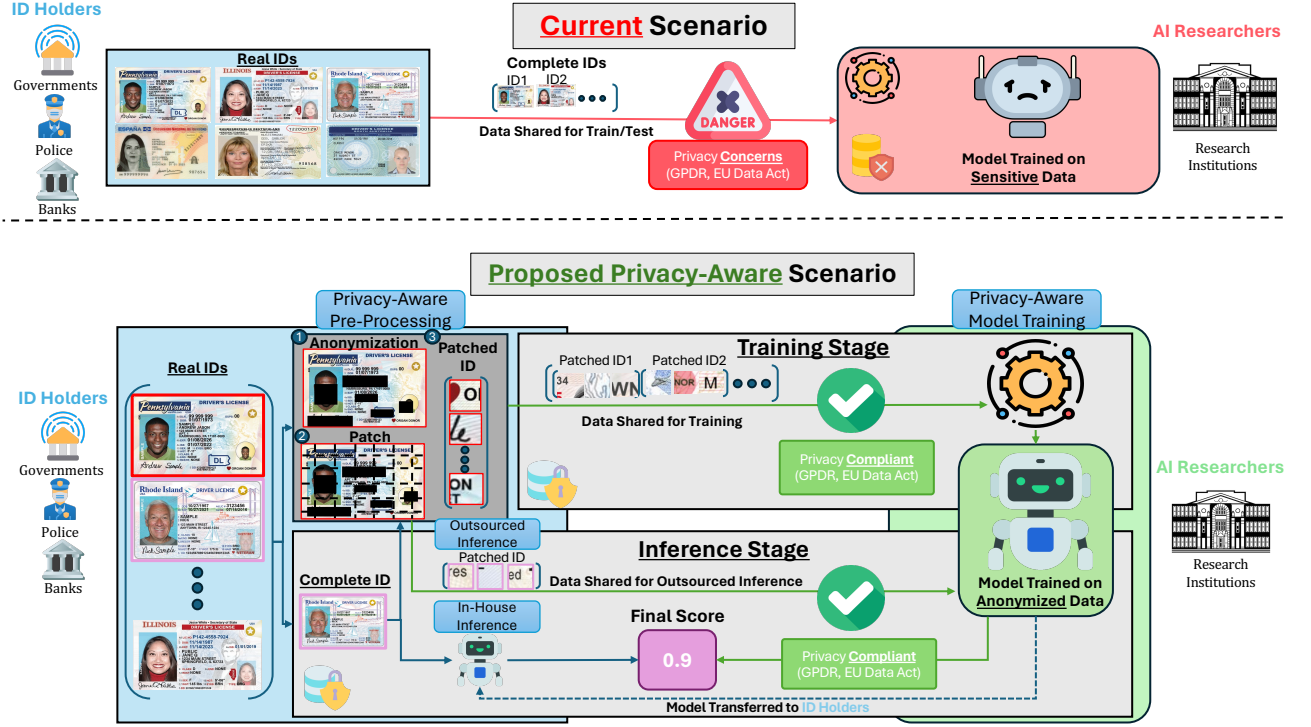


Figure 2: Our proposed framework for privacy-aware fake ID detection. The current scenario (top) raises privacy concerns regarding data regulations, and the need for complete ID sharing between ID Holders and AI Researchers. Our framework proposes a scenario where collections of non-ordered patches extracted from different levels of anonymized IDs can be used to preserve the sensitive information of ID owners during data sharing for training and inference in both in-house and outsourced schemes.

important concerns in terms of attacks, e.g., if the attackers are able to access the model trained on whole ID private data, they could use techniques that retrieve training data with small prior information about the data distribution [9, 13, 40].

Our proposed privacy-aware scenario is based on the premise that an individual patch contains much less sensitive information than the whole ID. In addition, to provide flexibility to the particular restrictions of each ID Holder, we explore different anonymization levels, removing patches from sensitive regions as desired. For example, ID Holders may request AI Researchers to train a fake ID detector but they may not want to share any personal information about the ID owners. As a result, ID Holders can anonymize the sensitive sections from an ID, depending on their preferences for the task at hand, and extract patches from the areas that hold non-anonymized information. Additionally, to increase privacy, the extracted patches can be randomized regarding the order in which they are shared with the AI Researchers, further preventing reconstruction. This flexibility allows for fruitful collaboration between ID Holders and AI Researchers to train fake ID detectors in any ID Holder restrictions.

Once the fake ID detector is trained by the AI Researchers, the ID Holders can decide whether inference is carried out inside the AI Researchers infrastructures or internally, as seen in Fig. 2. For example, if ID Holders want to



perform in-house inference using sensitive information that they only have access to, AI Researchers can transfer the fake ID detector previously trained using anonymized IDs to ID Holders. However, if ID Holders do not have such resources; they can rely on the AI Researchers for inference, since the ID Holders always control the amount of sensitive information shared for each ID. The proposed scenario can also be applicable to the research community in order to advance in this challenging topic, since research groups can share patches of IDs, including different levels of anonymization as desired.

The main contributions of the present study are as follows:

- We propose and explore a new methodology to facilitate the collaboration between ID Holders and AI Researchers for advancing real-world fake ID detection. Concretely, instead of feeding the fake ID detectors with the whole ID, as is commonly done in the literature, we explore privacy-aware scenarios based on different patch sizes ( $64 \times 64$  and  $128 \times 128$ ) and anonymization configurations (non-, pseudo-, and fully-anonymized ID). This proposal increases flexibility to both ID Holders and AI Researchers for both the training and inference stages, as shown in Fig. 2. Depending on the particular restrictions of the ID Holder, different setups can be selected to trade-off and optimize both privacy and performance.
- We provide a new database, FakeIDet2-db, which contains official real data, along with *print*, *screen*, and *physical composite* attacks. To our knowledge, FakeIDet2-db is the first database containing physical composite forgeries, as previous ones considered digital composites. In total, FakeIDet2-db comprises 922,057 patches extracted from 2,000 ID images (pseudo- and fully-anonymized configurations) from 47 different Spanish IDs. In addition, to increase the variability during the acquisition, we consider three smartphones for different end-users, including different hardware and software: iPhone 15 (high-end), Xiaomi Mi 9T Pro (medium-end) and Redmi 9C NFC (low-end). To add further variability, images are taken at 3 different heights (10 cms, 12.5 cms, and 15 cms) with respect to the ID and also different illumination conditions: *no-light* with the camera flash activated, *dim-light* with/without the camera flash activated, and *bright-light* with/without the camera flash activated.
- We propose a novel privacy-aware fake ID detector, FakeIDet2, which introduces two new learnable modules: the Patch Embedding Extractor and the Patch Embedding Fusion. The Patch Embedding Extractor leverages the DINOv2 foundation model to learn representations of individual patches from real/fake IDs, using an optimized AdaFace loss function [17] through adaptable class weights, which evolve as training progresses [14]. Once the embeddings have been obtained, they are merged jointly in the Patch Embedding Fusion module.
- We have developed a standard reproducible benchmark on which we evaluate the performance of our proposed FakeIDet2 in 3 different ID databases (DLC-2021 [30], KID34K [28], and Benalcazar *et al.* synthetic database of [5]), considering both physical and synthetic attacks, with the goal of assessing the performance in realistic out-of-distribution data. The proposed FakeIDet2-db and benchmark will be publicly available for reproducibility

reasons in our GitHub repository<sup>5</sup>, allowing a straightforward comparison of recent approaches with the state of the art.

A preliminary analysis of this privacy-aware scenario was conducted in [25]. The present article significantly improves [25] in the following aspects: *i)* We present our new publicly available FakeIDet2-db, which increases the number of unique real IDs (47 subjects) along with triple number of acquisition devices (now 3), illumination settings (now 3) and heights (now 3), resulting in 922,057 patches extracted from 2,000 ID images (pseudo- and fully-anonymized configurations). *ii)* We include physical composite attacks in our novel FakeIDet2-db. To our knowledge, this is the first database that includes this kind of Presentation Attack Instrument (PAI). *iii)* We propose a novel approach for fake ID detection, FakeIDet2, which overcomes the limitations in patch-level fusion encountered in FakeIDet [25]. While FakeIDet performs a simple mean of scores assigned to each individual patch, FakeIDet2 comprises two learnable modules (i.e., Patch Embedding Extractor and Patch Embedding Fusion) to leverage the fusion of learned patch representations, depending on the visual characteristics from real/fake IDs. The representations at patch level are obtained through an optimized version of AdaFace [17], including dynamic class weights, which accounts for the severe class imbalance present in the databases for the different PAIs. The fusion of the representations is performed through Multi-Head Self-Attention (MHSA), which ponders the embedding values based on the relations between them, to then compress them into a single embedding, through attention pooling based on [4]. The impact of these improvements can be seen in the results (Sec. 6). And *iv)* In order to advance in this research field, we propose a standard public benchmark considering a wide variety of physical and synthetic attacks from different databases in the literature, allowing a direct comparison of recent approaches with the state of the art.

The remainder of the paper is organized as follows. Sec. 2 provides an overview of the fake ID detection problem. In Sec. 3 we present our FakeIDet2-db, delving into the acquisition process for capturing real IDs and their fake counterparts. Sec. 4 introduces our novel privacy-aware fake ID detection method, FakeIDet2. Sec. 5 proposes a reproducible experimental protocol and standard benchmark, considering experiments in both intra- and cross-database scenarios. Finally, Sec. 6 analyzes the performance of our proposed fake detector using the proposed experimental protocol and standard benchmark and Sec. 7 draws the final conclusions.

## 2. Related Work

This section provides an overview of the fake ID detection problem. Sec. 2.1 provides a revision of the databases considered in the field. Sec. 2.2 focuses on representative fake ID detectors and recent international challenges. Finally, we summarize key aspects in Sec. 2.3.

### 2.1. Databases

Table 1 provides a summary of the most relevant public/private databases in the field of fake ID detection. One of the first family of databases was the

---

<sup>5</sup><https://github.com/BiDALab/FakeIDet2-db>

Database	#Samples	#IDs	#Devices	#PAIs	Official Real IDs?	Public?
BID (2020) [33]	28,800	28,800	N/A	8	✗	✓
DLC-2021 (2021) [30]	1,424 (videos)	1,000	2	4	✗	✓
Mudgalgundurao <i>et al.</i> (2022) [24]	97,477	433	N/A	2	✓	✗
Benalcazar <i>et al.</i> (2023) [5]	3,000	3,000	Synthetic	1	✗	✓
KID34K (2023) [28]	34,662	92	12	3	✗	✓
IDNet (2024) [39]	837,060	837,060	Synthetic	7	✗	✗
Open-Set (2024) [20]	5,424	N/A	Synthetic	2	✗	✓
Gonzalez <i>et al.</i> (2025) [15]	190,000	190,000	N/A	5	✓	✗
FakeIDet-db (2025) [25]	90	30	1	2	✓	✓
<b>FakeIDet2-db (proposed)</b>	2,000	47	3	3	✓	✓

Table 1: Summary of databases considered in the literature for research in fake ID detection. We indicate whether the databases are available or not for public research.

MIDV family [1, 6, 7]. With the original purpose of Optical Character Recognition (OCR), Bulatov *et al.* synthetically created a set of physical fake IDs, passports, and driving licenses. They used several digital templates from multiple countries that they filled with names and addresses from Wikipedia and artificially generated faces. As different versions of the database were released, the number of fake samples increased. The DLC-2021 database [30] used the documents of the MIDV-family to create PAIs: *color print*, *gray print*, and *screen*. The authors also provided “real” samples, although they should be considered fake samples as they are just high-quality prints built by them, not official IDs. A similar work is presented in the KID34K dataset [28], where Park *et al.* introduced a dataset of 34,000 images from 82 Korean IDs and driving licenses. As in the MIDV family, the authors claimed to release “real” samples, but they were also built by the authors, not official documents. In order to prove the quality of the “real” samples, they trained a Convolutional Neural Network (CNN) on the KID34K dataset using the whole ID. The evaluation was performed using official Korean IDs and “real” documents. After that, the authors applied a dimensionality reduction technique to visualize the model’s embeddings in 2D, where they showed that embeddings from both official and “real” generated IDs from the KID34K database were similarly distributed in the embedding space. These results raise questions about the fake ID detection problem, since fake IDs can be generated with such a resemblance to real ones that deep-learning models may not be able to extract distinguishable features for proper PAD. Soares *et al.* [33] introduced the Brazilian Identity Document (BID) database with a total of 28,800 images from Brazilian IDs that were digitally altered using different algorithms that removed blur and replace different personal information from the real IDs to comply with data privacy regulations. In [15], Gonzalez and Tapia proposed a more sophisticated attack procedure, i.e.,

printing the digital copy on a Poli-Vinyl Chloride (PVC) card, which resembles even more the appearance of real IDs.

Regarding synthetic data, Benalcazar *et al.* proposed in [5] to use Generative Adversarial Networks (GANs) to produce synthetic Chilean IDs. The proposed GAN was trained using only real Chilean ID samples. Although the data synthesized by the authors are not strictly real (and can be detected using GAN traces [26]), this was presented as a good idea to partially cover the lack of real data, for example, as a data enhancement strategy in training. Another synthetic database is IDNet [39], where Xie *et al.* proposed a database that comprises synthetic copies of IDs from 10 countries and 10 states of the United States of America. Given an ID template, the portrait images and the owners’ data were synthetically generated, with special care that the fields corresponded to the gender and age of the synthetic portrait image. In addition, the authors created six different types of digital manipulations, including inpainting [8], field cropping, and face morphing. A total of 837,060 IDs were generated, making it the largest and most diverse to date, although real data are not included. Markham *et al.* [20] developed Open-Set, a database that leverages neural style transfer, via GANs-based models to transfer textures from *print* and *screen* attacks to “real” images from the MIDV-2020 and DLC-2021 databases, creating even more samples of attacks.

## 2.2. Fake ID Detection Methods and International Challenges

One of the first methods for the detection of fake IDs was presented in [24], where the authors trained a CNN by pixel classification using an internal database, reporting a 2.22% EER. Gonzalez and Tapia proposed in [15] a two-stage system which first used a neural network to evaluate if the ID is real or fake, evaluating digital PAIs of type *composite* and *synthetic*. The second network classified the ID between real or fake, evaluating physical PAIs such as *print*, *display*, and *PVC*. When concatenating both systems, the Bona-fide Presentation Classification Error Rate at a fixed decision threshold  $\tau = 0.01$  (BPCER<sub>100</sub>) was 0.92%.

A corroboration that the fake ID detection field is receiving increasing attention in recent years is the organization of international challenges at top conferences. The first challenge was introduced at IEEE IJCB 2024 [34]. The organizers did not provide data to prepare the competition, and the fake ID detectors submitted were evaluated on real IDs. The winner of the challenge achieved an EER of 21.87%. The second edition of this challenge has been hosted at IEEE IJCB 2025<sup>6</sup>, where the organizers proposed two tracks. The first track considered IDs created by the organizers using PVC cards as “real” documents, the rest as attacks, and the second track treated only official IDs as real. Only for the first track, a database was given to the participants. The winner of the first track reported an EER of 11.34%, while for the second track, the best team reported an EER of 6.36%, but the second and third teams reported EERs of 23.87% and 31.94%, respectively. These results show that this is a very challenging task, especially because of the lack of public real data. More recently, the first challenge including digital manipulations for fake ID detection (DeepID

---

<sup>6</sup><https://sites.google.com/view/ijcb-pad-id-card-2025/>

challenge) has been organized at IEEE/CVF ICCV 2025<sup>7</sup>. This challenge proposed two tracks: one for binary classification focused on PAD (i.e., detecting fake and real documents) and one for localization (i.e., providing a mask showing the tampered sections). The organizers provided a database for all participants, named FantasyID, which contained fake templates from different countries from different regions of the world. The “real” ID data was created by printing high quality fakes using PVC cards and taking images of them. After that, those images were digitally altered through face-swapping and text-inpainting methods. For the detection track, the evaluation was performed using the F1 score with a decision threshold fixed at  $\tau = 0.5$  on two datasets: the FantasyID evaluation set, which contained PAIs that were not available in the training set, and a private dataset provided by the company PXL Vision, with the same type of attacks as in the FantasyID dataset, but using official IDs as real. The final score, named Aggregated F1 score, was a pondered mean that gave more importance to the F1 score obtained over the private dataset, hence benefiting models that generalized better to out-of-distribution data. The winning team achieved an Aggregated F1 score of 0.8, obtaining an F1 score of 0.99 and 0.72 in both the FantasyID dataset and the private dataset, respectively. These results, although impressive, show that there is a present issue in domain adaptation between official real IDs and fake samples created under laboratory conditions that are considered “real”. Hence, providing privacy-aware mechanisms that allow sharing more realistic ID data without compromising individual’s personal information is fundamental to further advance in this research field.

### 2.3. State of the Art: Summary

A clear trend can be observed on the basis of previous sections. Public databases in the literature do not have official real data available, and fake ID detectors trained using private databases with real data do not release the code or the weights to the research community, making it impossible to perform fair comparisons among state-of-the-art methods. Moreover, the characteristics of these databases are not always detailed (e.g., acquisition devices or number of unique IDs), which makes it even more difficult to advance in the field. The present study aims to advance through the following key contributions: *i*) the release of a new database, FakeIDet2-db, increasing the number of images from real and fake IDs, *ii*) the inclusion of a new kind of PAIs, named *physical composite*, to the proposed database, being the first one that contains this kind of attack, *iii*) a novel method for privacy-aware fake ID detection based on fusion of representations from individual patches, and *iv*) a new standard public benchmark that considers a wide variety of physical and synthetic attacks included in other public databases in the literature, considering IDs with different templates and demographic regions.

## 3. Proposed Database: FakeIDet2-db

This section describes our new FakeIDet2-db. Concretely, Sec. 3.1 and Sec. 3.2 provide all the details of the real and fake ID acquisition, whereas

---

<sup>7</sup><https://deepid-iccv.github.io/>

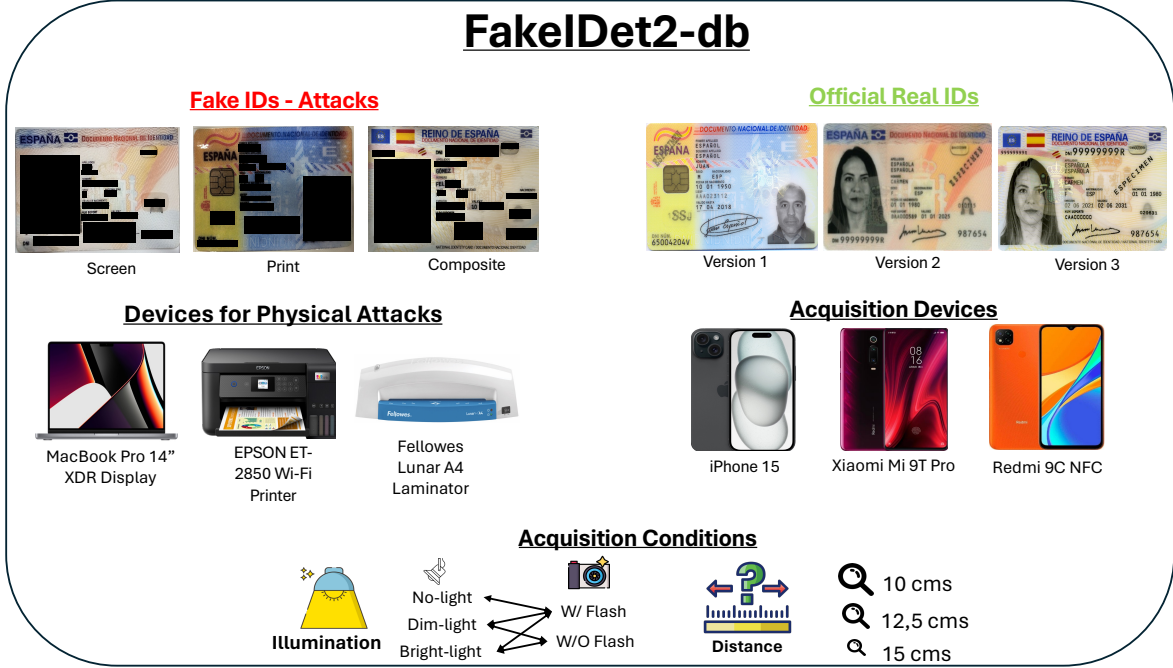


Figure 3: Main characteristics of our proposed public FakeIDet2-db. For the Fake IDs - Attacks, the personal information is redacted in this figure to protect the privacy of the subjects. Official Real IDs are based on template examples.

Sec. 3.3 describes the post-processing carried out for the different anonymization and patch size configurations.

### 3.1. Acquisition Setup: Real IDs

Fig. 3 summarizes the main characteristics of our proposed FakeIDet2-db. Regarding the number of unique IDs, our database comprises 47 different official Spanish IDs. The appearance of Spanish electronic IDs has changed over the years, which is a key aspect that has also been considered when capturing this database, including three different versions (see the Official Real IDs in Fig. 3). For the acquisition, we used three different smartphone models (Apple iPhone 15, Xiaomi Mi 9T Pro, and Redmi 9C NFC), to cover the range of sensor quality from high-end to low-end, respectively. Their main technical specifications are provided in Table 2 where we can see that both iPhone 15 and Mi 9T Pro have main camera sensors with 48MP while the Redmi 9C NFC only has 13MP. The iPhone camera is the best in terms of adaptability to low-light scenarios, given its aperture of  $f/1.6$ , although the Mi 9T Pro is close with an aperture of  $f/1.75$ . However, the Redmi 9C NFC struggles in these kind of low-light scenarios, since its aperture is greater,  $f/2.2$ . Regarding image resolution, the iPhone 15 is able to shoot ProRes images up to 8K resolution, but for our acquisition process, we set it to 4K, since both the Mi 9T Pro and the Redmi 9C NFC can only shoot images at that resolution. The photos of IDs were taken using a 4:3 aspect ratio. Three different heights were considered with respect to the document's vertical: 10 cms, 12.5 cms, and 15 cms, on a 3D printed adjustable platform that we developed specifically for this research. This platform enabled acquiring IDs

Feature	iPhone 15	Mi 9T Pro	Redmi 9C NFC
<b>Main Sensor</b>	48 MP (1/1.28")	48 MP (1/2")	13 MP (1/3.1")
<b>Aperture</b>	$f/1.6$	$f/1.75$	$f/2.2$
<b>Resolution</b>	4,032×3,024	4,032×3,024	4,032×3,024
<b>ISP / SoC</b>	Apple A16	Snapdragon 855	Helio G35
<b>Pixel Size</b>	1.22 $\mu\text{m}$ /2.44 $\mu\text{m}$	0.8 $\mu\text{m}$ /1.6 $\mu\text{m}$	1.12 $\mu\text{m}$

Table 2: Technical specifications of the smartphones considered in FakeIDet2-db.

precisely, similar to [24], where they captured IDs using a mobile application that provided a template in the camera preview to match the ID borders.

To provide realistic variability, we also considered different light conditions in terms of room illumination: *i) no-light*, with the camera flash activated, *ii) dim-light*, with images taken with/without the camera flash activated, and *iii) bright-light*, with images taken with/without the camera flash activated.

Therefore, given the variability factors mentioned above, for a unique ID, we obtained 45 images (i.e., 3 smartphones  $\times$  3 heights  $\times$  5 light conditions) covering different conditions, generating a total of 2,115 (i.e.,  $47 \times 45$ ) images of real IDs.

### 3.2. Acquisition Setup: Attacks

Fig. 1 shows visual examples of physical attacks (print, screen, and physical composite) available in our proposed FakeIDet2-db. Note that personal information is redacted in the figure of the article to protect the privacy of the subject.

To manufacture the print attacks, we used an HP ScanJet 8270 scanner at 600 Dots Per Inch (DPI), creating a digital copy of the real ID. After that, we printed the fake IDs using an EPSON ET-2850 Wi-Fi printer and laminated them to improve the realism using a Fellowes Lunar A4 thermal laminator, providing print attacks with the characteristic glossy texture of real IDs. The acquisition process was the same as for real IDs, yielding a total of 2,115 images for print attacks.

For screen attacks, we used a MacBook Pro 14" XDR screen, where the 2,115 images of real documents were displayed in full-screen and covering the whole smartphone camera preview. To increase variability between smartphone devices, each image was displayed and then captured using a randomly selected smartphone, ensuring that approximately one third of the images were taken with each device.

Regarding physical composite attacks, we cut sensitive sections from print attacks and placed them in the sensitive areas of the real IDs. Regarding privacy considerations, we only cut the date of birth, the name, and both surnames from the ID owner along with partial sections of the ID's number. To provide even more variability, some physical composite attacks were created using cut-outs of several print attacks. The cutouts of sensitive sections from a print attack were never displayed at the same time, further protecting the sensitive information of the ID owner. Additionally, we did not use the ID owner's portrait image, as it is sensitive information that cannot be shared under any circumstances. After that, we captured composite attacks following the same procedure as for





Figure 4: Examples of the different anonymization levels considered in the present study.

real IDs, described in Sec. 3.1, balancing the number of images of real and all types of attack across the database to 2,115.

Gathering all images from real and fake IDs, our database contains 8,460 total IDs images. From them, we selected 1,000 images, balancing them across different types of attacks and bona fide data (250 samples per class), different capture devices, and different illumination and height conditions. This subsampling aimed to avoid including images of real and fake IDs under all acquisition conditions, ensuring that fake ID detectors do not rely on superficial cues, such as illumination patterns, to distinguish between real and fake IDs, which could lead to overfitting.

### 3.3. Post-Processing: Anonymization and Patch Extraction

Fig. 4 provides graphical examples of the different anonymization configurations explored in the present study to facilitate collaboration between ID Holders and AI Researchers in real-world fake ID detection scenarios. The criteria followed to remove sensitive information at each anonymization configuration are the following:

1. *Non-Anonymized*: no sensitive sections are anonymized, so all information is available to detect real/fake IDs.
2. *Pseudo-Anonymized*: partial sections with sensitive information of real/fake IDs is displayed. This kind of anonymization is consistent along all images from the same ID, so no reconstruction is allowed.
3. *Fully-Anonymized*: all sensitive sections of real/fake IDs are completely anonymized.

Referring to *pseudo*- and *fully*-anonymized configurations, we used EasyOCR<sup>8</sup> and the GNU Image Manipulator Program (GIMP) to cover the sensitive regions with pitch black rectangles (with the color code (0,0,0) in the RGB spectrum). Since we had two levels of anonymization applied to the original, non-anonymized images, we obtained 2,000 images of real and fake IDs. Given that we had several images taken from the same ID, we took special care to cover the same partial sensitive sections across all images in the pseudo-anonymized configuration. Once all IDs were anonymized, we processed them and extracted patches using PyTorch’s `unfold` method, specifying the same step and stride size as the patch size to avoid overlapping. Patches with a pitch black content

<sup>8</sup><https://github.com/JaidedAI/EasyOCR>

		Real	Print	Screen	Composite
Patch Size	Anon. Level				
$128 \times 128$	Non-Anon	56,017	52,976	55,927	3,810
	Pseudo-Anon	32,875	28,432	32,170	1,805
	Full-Anon	21,896	20,363	21,474	1,216
$64 \times 64$	Non-Anon	222,622	211,396	221,610	7,931
	Pseudo-Anon	152,612	132,920	148,599	6,297
	Full-Anon	110,162	101,178	107,104	2,954

Table 3: Number of patches per real/fake ID, patch size, and anonymization level considered in our proposed FakeIDet2-db.



Figure 5: Graphical samples of real/fake patches extracted from different IDs. Real patches (first column, green color), are shown along the different types of attacks in the proposed database (second, third, and fourth columns, red color), at both  $128 \times 128$  and  $64 \times 64$  sizes.

greater than 80% were discarded and the remaining were kept with a sampling probability of  $p = 0.9$  to further prevent reconstruction. After that, for each ID image, we created a folder where the extracted patches were stored using random numbers of six figures as the filename of the patch (e.g., 762542.jpeg), so no spatial layout could be inferred.

An important point is the number of patches available with respect to anonymization and patch size configurations, which are depicted in Table 3 for real IDs and the different attacks considered. For example, the Full-Anon,  $128 \times 128$  configuration shows a noticeable drop in terms of the number of patches compared to the Non-Anon,  $64 \times 64$  configuration, which has almost ten times fewer patches. As we plan to release FakeIDet2-db, the pseudo- and fully-anonymized ID configurations at  $128 \times 128$  and  $64 \times 64$  patch sizes will be available for privacy reasons, as proved in the results section (Sec. 6) that these privacy-aware scenarios are very useful to facilitate collaborations between ID Holders and AI Researchers. If we consider the number of patches from the said configurations, a total of 922,057 patches extracted from 2,000 images will be available to researchers to train and benchmark their proposed fake ID detectors.

For completeness, Fig. 5 shows different examples of real/fake patches extracted from different IDs. One can see that the  $128 \times 128$  patch size contains

much more information compared to their  $64 \times 64$  counterparts. Some small traces can be observed in the different attacks. For example, composite attacks might show the change in color and texture between the background and the altered section in the foreground. However, patches from screen attacks might show subtle traces of the characteristic Moiré patterns.

#### 4. Proposed Method for Fake ID Detection: FakeIDet2

Our proposed fake ID detection method, FakeIDet2, proposes a privacy-aware, patch-level representation fusion [14]. Fig. 6 provides a graphical representation of FakeIDet2. This comprises three main modules: the Privacy-Aware Patch Extractor, the Patch Embedding Extractor, and the Patch Embedding Fusion. The Privacy-Aware Patch Extractor module receives a complete ID, considering any anonymization level presented in Sec. 3.3. This first module divides the entire ID into patches, removing sensitive information if applicable (i.e., the regions of the ID that are blacked out). After that, those patches are forwarded to the Patch Embedding Extractor, which uses a fine-tuned DINOv2 as a feature extractor to learn discriminative features at the patch level of each type of PAI, providing an embedding for each patch. Then, those embeddings are treated as tokens, and passed into a MHSA layer, which ponders the embeddings values depending on their importance in the sequence. After that, an attention pool layer selects discriminative features from the sequence, obtaining a single embedding, which is forwarded to a Multi-Layer Perceptron (MLP) that yields a final score per ID, indicating whether it is real or fake. Next, we describe the technical details of the *learnable* modules of FakeIDet2.

##### 4.1. Patch Embedding Extractor

To effectively learn features at patch level, we go deep into representation learning, aiming to obtain compressed, meaningful representations from high-dimensional data into the embedding space. To do so, we treat patches coming from both real and fake IDs as four different classes (i.e., 3 PAIs + real) and use DINOv2’s (ViT-S/14) [27] backbone with its weights frozen. Using DINOv2 for extracting patch embeddings seems appropriate, since the goal of its original training procedure was to match the embedding distribution between images where the full context is given and random patches extracted from the same image. To take advantage of these features, we attach a final layer to DINOv2 embeddings; hence, our Patch Embedding Extractor is defined as an encoder function that maps an input patch  $x_i \in \mathbb{R}^{p \times p \times c}$ , where  $p$  is the patch size and  $c$  is the channel dimension (i.e.,  $c = 3$  in the RGB spectrum), to its corresponding compressed representation  $z_i \in \mathbb{R}^d$ , where  $d$  is the dimension of the embedded space.

We explore three softmax-based loss functions [23]: CosFace [38], ArcFace [11], and AdaFace [17], to assess which one best fits our problem to learn discriminative representations. The generic formulation for the softmax loss function is defined in Eq. 1, where  $C$  is the number of classes,  $f(\theta_{y_i})$  is a function that computes the alignment between the embedding obtained from the input image and the class prototype of its label  $y_i$  and  $s$  is a scaling factor that modulates the alignment value. Hence, the objective for an embedding of one class is to be as close as possible to other embeddings from the same class (better aligned) while

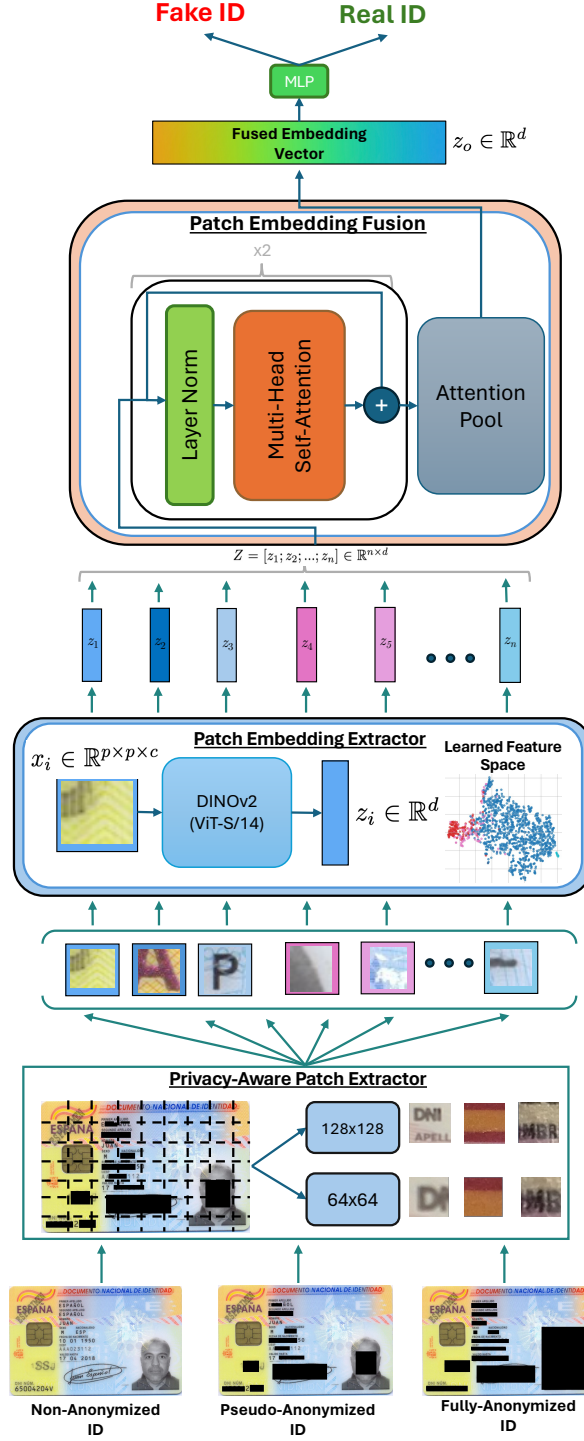


Figure 6: General diagram of our proposed fake ID detector, FakeIDet2. Our proposal has three different stages: *i*) the entire ID is forwarded to the Privacy-Aware Patch Extractor, extracting patches of fixed size (128×128 or 64×64); *ii*) those patches are forwarded into the Patch Embedding Extractor, which yields an embedding per patch; and *iii*) finally, those embeddings are used at the Patch Embedding Fusion module to generate a single embedding which is used by an MLP, providing a final score that is thresholded to obtain the final decision: real or fake ID.

being apart from embeddings of other classes by an imposed distance, called margin (worst aligned). The main differences between these loss functions reside in the way the margin is computed for the alignment function,  $f(\theta_{y_i})$ . For example, CosFace, defined in Eq. 2, computes the loss by adding the margin  $m$  to the cosine similarity, while ArcFace, defined in Eq. 3, computes the loss by adding an angular margin  $m$  to the cosine similarity. In the case of AdaFace, defined in Eq. 4, the margin is adaptively calculated, depending on the quality of the image [31], which is calculated as the embedding norm obtained from the input image normalized on batch statistics for better stability and is denoted by  $\|\hat{z}_i\|$ .

$$\mathcal{L} = \log \left( \frac{\exp(f(\theta_{y_i}))}{\exp(f(\theta_{y_i})) + \sum_{j \neq y_i}^n \exp(s \cos \theta_j)} \right) \quad (1)$$

$$f(\theta_{y_i})_{\text{CosFace}} = \begin{cases} s \cos(\theta_j - m) & j = y_i \\ s \cos(\theta_j) & j \neq y_i \end{cases} \quad (2)$$

$$f(\theta_{y_i})_{\text{ArcFace}} = \begin{cases} s \cos(\theta_j + m) & j = y_i \\ s \cos(\theta_j) & j \neq y_i \end{cases} \quad (3)$$

$$f(\theta_{y_i})_{\text{AdaFace}} = \begin{cases} s \cos(\theta_j + (-m \cdot \|\hat{z}_i\|)) - (m \cdot \|\hat{z}_i\| + m) & j = y_i \\ s \cos(\theta_j) & j \neq y_i \end{cases} \quad (4)$$

An issue we encountered when training the Patch Embedding Extractor was that softmax-based loss functions did not account for the severe class imbalance in the physical composite attacks (see Table 3). To address this limitation, we propose to apply dynamic class weights to these loss functions that evolve as training progresses [14]. The initial weights  $w_0 \in \mathbb{R}^C$ , where  $C$  is the number of classes, are calculated as the normalized inverse of the frequency for each class using Eq. 5, where  $N$  is the total number of patches in the database and  $N_i$  is the total number of patches belonging to the  $i$ -th class.

$$w_0 = \begin{bmatrix} \frac{N}{N_1} \\ \frac{N}{N_2} \\ \dots \\ \frac{N}{N_C} \end{bmatrix} \times \sum_{i=1}^C \frac{C}{N_i} \quad (5)$$

After that, the class weights are updated at each epoch until they all converge to 1, hence progressively giving the same weight to all classes. The update rule is presented in Eq. 6, where  $w_t \in \mathbb{R}^C$  is a vector that stores the weights of the class at the time step  $t$ ,  $\mathbf{1} \in \mathbb{R}^C$  is a vector full of ones,  $\lambda_t \in [0, 1]$  is a pondering factor that linearly decays from 1 to 0 as training progresses, and  $e$  is the total number of time steps involved in the training procedure and  $\lambda_e = 0$ . Intuitively, at the beginning of the training, the class weights will be close to  $w_0$ , giving more importance to the underrepresented class, but, as time goes by, the class

weights will be closer to 1, giving all classes the same importance at the end of the training.

$$w_t = (1 - \lambda_t)\mathbf{1} + \lambda_t w_0, \quad \lambda_t \leftarrow \lambda_0 + (\lambda_e - \lambda_0) \times \left(\frac{t}{e}\right) \quad (6)$$

These class weights are then used to modulate the gradient signal that the margin loss function produces, giving higher values when the embeddings of the underrepresented class are close to the embeddings from another class. The modified version of this loss is defined in Eq. 7, where  $\mathcal{L}$  is the loss function defined in Eq. 1,  $w_{t,y_i}$  is the class weight associated with the label  $y$  of the  $i$ -th element of the batch at the time  $t$ .

$$\mathcal{L}_{\text{weighted}} = -w_{t,y_i} \cdot \mathcal{L} \quad (7)$$

#### 4.2. Patch Embedding Fusion

To effectively fuse all patch embeddings of a given ID, we use a Multi-Head Self-Attention (MHSA) layer [10]. This self-attention mechanism was introduced to solve problems related to long-range dependency issues of the model, which are typical in Recurrent Neural Networks (RNN) models, which process information sequentially. However, in the self-attention mechanism, all elements of the input sequence are processed at the same time, enabling modeling of dependencies from distant tokens. The Self-Attention layer expects as input a sequence of embeddings (or tokens)  $X \in \mathbb{R}^{n \times d}$ , where  $n$  is denoted as the sequence length and  $d$  the embedding dimension. The sequence is processed according to the Self-Attention mechanism, defined in Eq. 8, where  $Q$  is the query,  $K$  is the key,  $V$  is the value, and  $d_k$  is the projected embedding dimension for the query and the key. The query, key, and value matrices are single linear projections of  $X$ , which are calculated as  $Q = XW_Q$ ,  $K = XW_K$  and  $V = XW_V$ , respectively, where  $W_Q \in \mathbb{R}^{d \times d_k}$ ,  $W_K \in \mathbb{R}^{d \times d_k}$  and  $W_V \in \mathbb{R}^{d \times d_v}$ , where  $d_v$  is the projected dimension of the value. Hence, the sequence obtained after the self-attention mechanism is a matrix  $X' \in \mathbb{R}^{n \times d}$  where each token value has been modified depending on their importance in the sequence, compared to their peers.

$$\text{Attention}(Q, K, V) = \text{softmax}\left(\frac{QK^\top}{\sqrt{d_k}}\right) V \quad (8)$$

Furthermore, the attention mechanism allows queries, keys, and values to be linearly projected  $h$  times using different learned projections of dimensions  $d_k$  and  $d_v$ . To achieve this,  $d_k$  and  $d_v$  are typically set to  $d/h$ , where  $d$  is the dimension of the model. Each of these computations defines an attention head (Eq. 9). The outputs of the  $h$  attention heads are concatenated and projected back to the original input dimension using a final linear transformation  $W^O \in \mathbb{R}^{hd_v \times d}$  (Eq. 10).

$$\text{head}_i = \text{Attention}(Q_i, K_i, V_i) \quad (9)$$

$$\text{MultiHead}(Q, K, V) = [\text{head}_1, \dots, \text{head}_h]W^O \quad (10)$$

Since the Patch Embedding Extractor produces an embedding  $z_i$  for each patch  $x_i$ , we treat the set of embeddings that come from a single ID as a sequence  $Z = [z_1; z_2; \dots; z_n] \in \mathbb{R}^{n \times d}$ , where  $n$  is the number of patches from a single ID and  $d$  is the dimension of the embedding obtained from the Patch Embedding Extractor. These embeddings are then normalized through layer normalization [3] and are transmitted to the MHSA layer that produces a feature sequence  $Z' = [z'_1; z'_2; \dots; z'_n] \in \mathbb{R}^{n \times d}$  where the embedding values  $z'_i$  have been modified according to their importance in the input sequence. Furthermore, we leverage residual connections to enable a better gradient flow in the training procedure, since two layers of MHSA and layer normalization are stacked in this module, where the first MHSA layer has  $h = 8$  attention heads and the second layer has  $h = 4$  attention heads.

Using the MHSA mechanism is beneficial for our proposed FakeIDet2 as: *i*) it leverages the patch embedding space learned by the Patch Embedding Extractor, and *ii*) it can detect elements of the sequence that may be anomalous, which is analogous to detecting tampered sections of a composite attack. Then, the feature sequence is forwarded into a temporal attention pool module, similar to [4], generating a single embedding  $z_o \in \mathbb{R}^d$ . Finally, we use  $z_o$  as an input to an MLP, comprising a single layer with sigmoid activation, obtaining a final score per ID.

## 5. Experimental Setup

In order to define a standard, reproducible benchmark that allows us to advance properly in this research field, in this section, we define our experimental setup. First, Sec. 5.1 describes the specific hyperparameters of our proposed FakeIDet2 method. Then, in Sec. 5.2 we describe the experimental protocol and the different scenarios of interest in the analysis. Finally, Sec. 5.3 describes the evaluation metrics. In general, we use the EER metric as a performance indicator to obtain the best patch and anonymization configuration. For all training procedures and experiments, we used only one NVIDIA RTX 3080 with 10GB of VRAM.

### 5.1. FakeIDet2: Hyperparameters

Regarding the Patch Embedding Extractor, for any patch size, the input is resized to  $224 \times 224$ , which is the input shape of DINOv2, with an embedding layer of dimension  $d = 128$ . We use Adam optimizer with weight decay, an initial learning rate  $\alpha_0 = 0.00125$ , and exponential decays for the momentum estimators of  $\beta_1 = 0.9$  and  $\beta_2 = 0.999$ , respectively, and a weight decay  $\delta = 0.0001$ . The modified versions of the softmax-based losses presented in Sec. 4.1 are defined with a margin of  $m = 0.4$ , which are the optimal experimental values that perform well for low-quality datasets without compromising the capacity in high-quality data, and a scaling factor of  $s = 64$ , as it provides a strong signal from both samples that are close and far from the decision boundary, creating better separability in the learned representations according to [17]. All models are trained for 70 epochs, with an early stopping condition that ends the



training if the loss in the validation does not decrease for 5 consecutive epochs. Furthermore, we use a cosine annealing decay scheduler for the learning rate, with values decreasing from  $\alpha_0 = 1.25e - 3$  to  $\alpha_e = 1.25e - 4$ , and a batch size of 256. Regarding data transformations, we opt to apply random Gaussian blur with a kernel size  $k = 3$  and color jitter with a brightness of 0.2, a hue of 0.05, a contrast of 0.25, and a saturation of 0.2. These data transformations are applied in training time with a probability of  $p = 0.2$ . Finally, the pixel values are normalized according to ImageNet mean and standard deviation statistics.

For the Patch Embedding Fusion, in particular the MHSA layers, we define a context length of 384 for both patch configurations, which is enough so that no patch from an ID is left out when performing a forward pass. Furthermore, we use masked-MHSA to indicate which embeddings should be attended, so that in case the number of patches from a single ID is fewer than the context length, the introduced padded embeddings are ignored. We use Binary Cross Entropy (BCE) loss with class weights, since there is a class ratio of 3 to 1 between the fake and the real data. For all of our experiments, we choose Adam as optimizer, using an initial learning rate  $\alpha_0 = 1.25e - 4$  and exponential decays for the momentum estimators of  $\beta_1 = 0.9$  and  $\beta_2 = 0.999$ , respectively, with 1 epoch of learning rate warm-up. Furthermore, the learning rate followed a cosine annealing decay from  $\alpha_0 = 1.25e - 4$  to  $\alpha_e = 1.25e - 5$ .

All configurations in terms of anonymization levels and patch sizes are trained for 10 epochs with a batch size of 4, selecting the best performing model for each training procedure according to the lowest validation loss achieved.

### 5.2. Experimental Protocol

In order to assess the feasibility of our proposed FakeIDet2 detector and privacy-aware scenarios to facilitate collaboration between ID Holders and AI Researchers, we propose an experimental protocol that aims to: *i)* evaluate FakeIDet2 performance regarding patch size and anonymization configurations in our new FakeIDet2-db, comparing the results with the traditional case in the literature, i.e., feeding the fake detectors with the whole non-anonymized ID, and *ii)* explore domain adaptation, by evaluating FakeIDet2 on popular databases in the topic of fake ID detection.

First, in all experiments that involve any kind of training procedure, the database is divided into a development set (80% of the real and fake IDs) and a final evaluation set (the remaining 20%) for all training scenarios. This split simulates a realistic scenario in which the evaluation involves unseen identities. In addition, for our FakeIDet2-db, the first version of Spanish ID is included only in the final evaluation set, not in the development set, to analyze the generalizability of FakeIDet2 to other ID templates.

Regarding the experiments included in Sec. 6, we first validate the technical details of our proposed FakeIDet2 in terms of performance and privacy. Sec. 6.1 explores the different softmax-based loss functions for representation learning, which will determine the best loss function for the Patch Embedding Extractor module. After that, an exploration in terms of the optimal patch size is conducted in Sec. 6.2, to test whether more patches at lower sizes (i.e.,  $64 \times 64$ ) yield better performance compared to fewer patches of greater size (i.e.,  $128 \times 128$ ). Additionally, we also compare the performance of our proposed FakeIDet2 in terms of anonymization levels in Sec. 6.3, which also goes deep into interesting scenarios such as how well a model trained on fully-anonymized data performs

on non-anonymized data. Finally, for completeness, we compare FakeIDet2 with our previous FakeIDet [25]. From this set of experiments, we will select the best configuration of FakeIDet2 in terms of privacy versus performance.

Then, after validating the technical contributions of FakeIDet2, we analyze its generalization capabilities against unseen scenarios, including leave-one-out experiments for two interesting scenarios: novel attack detection and out-of-distribution sensors. In this case, we train FakeIDet2 with the optimal configuration, leaving images belonging to one PAI or images taken from one sensor out of the training data, testing the performance of FakeIDet2 when exposed to unseen attacks, or images taken from acquisition devices with sensors that were not used during training. The analyses of these scenarios are available in Sec. 6.4 and Sec. 6.5, respectively.

Finally, we evaluate in Sec. 6.6 the best configuration of FakeIDet2 in a cross-database scenario, providing a standard public benchmark for the research community. This scenario aims to evaluate our proposed model using unseen databases, where the IDs are from different countries, including different templates, and are acquired under different conditions in terms of illumination and acquisition devices. In addition, these databases contain different PAIs compared to our proposed database. With this goal in mind, we select three different databases for performance evaluation, DLC-2021 [30], KID34K [28] and Benalcazar *et al.* [5]. These databases are selected for the following reasons: *i*) each database has ID images from three different regions of the world (i.e., Europe, Asia and South America); hence the evaluation is conducted on different distributions in terms of ID templates with different alphabets, and *ii*) we contemplate physical attacks as well as synthetic attacks in our evaluation, to assess the performance of FakeIDet2 to synthetic data in the form of fake IDs.

### 5.3. Evaluation Metrics

Similar to previous approaches presented in the literature [34], we adopt the ISO/IEC 30107-3 standard<sup>9</sup> for the evaluation of fake ID detection technology. This includes the use of the Bona-fide Presentation Classification Error Rate (BPCER) and Attack Presentation Classification Error Rate (APCER) metrics. The BPCER measures the proportion of bona fide samples (i.e., real IDs) that are incorrectly classified as attacks (i.e., fake IDs), see Eq. 11, where  $N_{BF}$  is the number of bona fide samples,  $RES_i$  is a term that is equal to 1 if the presented sample is incorrectly classified as an attack, and  $\tau$  is the operational point, i.e., the threshold used to classify a sample as bona fide if the confidence of the prediction goes below and as an attack otherwise.

$$BPCER(\tau) = \frac{\sum_{i=1}^{N_{BF}} RES_i}{N_{BF}} \quad (11)$$

Similarly, APCER quantifies the proportion of attack samples (i.e., fake IDs) that are misclassified as bona fide (i.e., real IDs):

$$APCER(\tau) = \frac{1}{N_{BF}} \sum_{i=1}^{N_{BF}} 1 - RES_i \quad (12)$$

---

<sup>9</sup><https://www.iso.org/standard/79520.html>

In addition, we consider the Equal Error Rate (EER), a widely used metric in the literature. The EER corresponds to the error rate at the operational threshold  $\tau$  where  $\text{BPCER}(\tau) = \text{APCER}(\tau)$ , providing a summary of the system performance in a single value.

## 6. Experimental Results

This section evaluates the performance of our proposed FakeIDet2. The performance results included in all tables are at the ID level, not the patch level, on the final evaluation datasets. This facilitates the comparison of our proposed FakeIDet2 with traditional approaches in the literature, focused on the whole ID level evaluation.

First, we evaluate the technical novelties of our proposal. Sec. 6.1 provides a comprehensive comparison in terms of softmax-based loss functions. The analysis of the optimal patch size configuration and anonymization level is carried out in Sec. 6.2 and Sec. 6.3, respectively. Finally, for completeness, we compare FakeIDet2 with our previous FakeIDet [25]. These first experiments are carried out using our new FakeIDet2-db, as described in Sec. 5.2.

Once the preliminary analysis is conducted using FakeIDet2-db, we select the optimal configuration balancing performance and privacy and use it to evaluate FakeIDet2 in two common scenarios for PAD. The first scenario is introduced in Sec. 6.4, which studies the performance of FakeIDet2 to unseen attacks. Hence, we train FakeIDet2 with the optimal configuration leaving one of the PAIs out of the training set. The second scenario, Sec. 6.5, analyzes the performance of FakeIDet2 when exposed to images taken with smartphone cameras that have not been seen in training. To do so, we train FakeIDet2 using images from all camera sensors except one. Finally, we evaluate in Sec. 6.6 the best configuration of FakeIDet2 in a cross-database scenario, providing a standard public benchmark for the research community.

### 6.1. Selecting the Optimal Loss Function Configuration

Given that different softmax-based loss functions are considered in FakeIDet2 training, we perform a comparison in terms of performance using the  $128 \times 128$ , Non-Anonymized configuration. For each loss function, we also compare our proposed dynamic class weights (Dynamic-Weights) described in Sec. 4.1 with traditional approaches considered in the literature:

- No-Weights: All classes have a fixed weight equal to one.
- Static-Weights: Each class has its own weight based on its frequency in the dataset (Eq. 5), which is kept fixed during training.

Table 4 shows the results for the different loss functions and different types of class weights during learning. We observe that for all loss functions, the proposed Dynamic-Weights achieve better overall results. For example, in the case of CosFace we see that the No-Weights and Static-Weights configurations achieve practically the same results with 4.32% EER, while the Dynamic-Weights improve performance to 3.66% EER. ArcFace shows minor improvements using Dynamic-Weights, with an improvement of 0.34% EER and 1.67% EER with respect to using Static-Weights and No-Weights, respectively. The

Model	Screen	Print	Composite	All
<i>CosFace</i> [38]				
No-Weights	3.00	1.00	6.12	4.32
Static-Weights	<b>1.02</b>	3.89	7.17	4.32
Dynamic-Weights	4.00	<b>0.00</b>	<b>4.08</b>	<b>3.66</b>
<i>ArcFace</i> [11]				
No-Weights	6.00	6.77	10.21	7.32
Static-Weights	5.08	5.83	8.17	5.99
Dynamic-Weights	<b>1.12</b>	<b>2.89</b>	<b>7.13</b>	<b>5.65</b>
<i>AdaFace</i> [17]				
No-Weights	6.23	<b>0.00</b>	4.08	3.66
Static-Weights	6.00	7.77	5.12	6.31
Dynamic-Weights	<b>1.23</b>	0.12	<b>2.09</b>	<b>2.01</b>

Table 4: Results in terms of EER (%) for the different loss functions (CosFace, ArcFace, and AdaFace) and different types of class weights during learning. The proposed Dynamic-Weights allow to deal with class imbalance among the different PAIs patches. Experiments are conducted on the entire evaluation set of FakeIDet2-db, considering the configuration 128×128 Non-Anonymized.

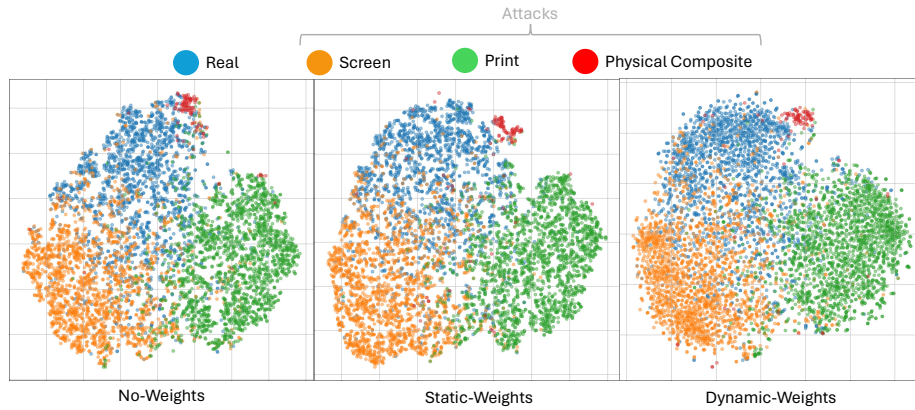


Figure 7: Differences of AdaFace’s learned embedding space using No-Weights (left), Static-Weights (middle), and Dynamic-Weights (right) via t-SNE 2D.

best performance is obtained with AdaFace using Dynamic-Weights, with 2.01% EER, providing an improvement of 1.65% EER over No-Weights, and 4.30% EER over Static-Weights.

Furthermore, in order to prove that the improvement in performance correlates with how the embedded space is modeled, we plot in Fig. 7 the embeddings distributions of AdaFace using the t-SNE projection in 2D. In the figure, we show visual examples when: *i*) No-Weights are applied (left), *ii*) Static-Weights are applied (middle), and *iii*) Dynamic-Weights are applied (right). The data used for this visualization were randomly sampled from the test set, comprising 6,000 patches.

In the No-Weights case, we observe that the physical composite patches (red

points) overlap with the real patches (blue points). This is a critical issue, as confusion between these two classes can significantly hinder the detection of physical composite attacks at the document level, indicating that the embeddings are not sufficiently discriminative.

For Static-Weights, we observe a clearer clustering trend for physical composite patches. However, as expected, keeping the weight values fixed throughout the training biases the model away from properly clustering patches from the other classes (i.e., real, print, and screen), which appear more scattered across the embedding space.

In contrast, with our proposed Dynamic-Weights, we observe a clear separation between physical composite patches and those from the remaining classes. This is enabled by the initial class weights computed at the start of training. Moreover, the clustering of the other classes is more consistent, with less sparsity in the boundaries between clusters and more sparsity within clusters compared to No-Weights and Static-Weights, which indicates a more robust feature extraction. We attribute this behavior to the later training stages using adaptive weights, which guide the model to better cluster patches from the more prevalent classes in the dataset.

The results of this section showcase that our proposed dynamic class weights approach better suits the problematic scenario of heavy class-imbalance. In summary, we adopt the AdaFace loss function with Dynamic-Weights for the rest of our experiments.

## 6.2. Patch Size vs. Performance

For this section, we consider the Non-Anonymized configuration in order to provide a direct comparison of our proposed FakeIDet2 approach, based on patches, with the current scenario in the literature, based on the entire Non-Anonymized ID. For completeness, we also include in the comparison our previous FakeIDet detector [25], trained using  $128 \times 128$  and  $64 \times 64$  patch sizes, similar to FakeIDet2. For the scenario of feeding the fake detector with the whole ID, we fine-tune the DINOv2 foundation model [27] using a final sigmoid layer attached to the DINOv2 output embedding.

Table 5 shows a comparison between the performance of the fine-tuned DINOv2 (whole ID), FakeIDet [25], and FakeIDet2 in terms of EER. In general, we see that training on the whole ID does not achieve good results (22.63% EER), in contrast to our proposed patch-wise approach.

In the  $128 \times 128$  configuration, we observe that FakeIDet2 performs better than FakeIDet in detecting fake IDs of type screen (1.23% vs. 7.10% EER) and composite (2.09% vs. 54.08% EER), and remains close to FakeIDet in detecting print fake IDs (0.12% vs. 0.00% EER). Furthermore, we observe that for the physical composite fake IDs, the performance of FakeIDet drops to 54.08% EER, while FakeIDet2 accurately detects these types of fake IDs using patch feature extraction and fusion, achieving a 2.09% EER. The performance drop is attributed to the way FakeIDet computes the document level score. Given all patches from a real or fake ID, it calculates a score per individual patch and fuses them all together using a simple average, which yields a final score at the document level. FakeIDet is reliable if the PAIs considered have the same patterns in the whole image. For example, in the case of a screen or print fake ID, it has the same properties throughout the whole ID (that is, traces

Model	Screen	Print	Composite	All
<i>Entire ID</i>				
DINOv2 [27]	21.85	11.35	24.68	22.63
<i>Patch Size: 128×128</i>				
FakeIDet [25]	7.10	<b>0.00</b>	54.08	25.58
<b>FakeIDet2</b>	<b>1.23</b>	0.12	<b>2.09</b>	<b>2.01</b>
<i>Patch Size: 64×64</i>				
FakeIDet [25]	9.00	<b>0.00</b>	58.17	26.25
<b>FakeIDet2</b>	<b>4.53</b>	1.45	<b>7.17</b>	<b>3.99</b>

Table 5: Performance results for the fine-tuned DINOv2 (Entire ID), FakeIDet [25], and proposed FakeIDet2 in terms of EER. Results are achieved using the evaluation set of FakeIDet2-db. The Non-Anonymized configuration (Entire ID) simulates current scenarios in literature.

or fingerprints of the fake ID), but this is not true for physical composite fake IDs, as the ID is mostly real with the exception of altered sections, failing to detect these types of fake ID properly. Finally, in the 64×64 configuration, we can observe a similar trend, although performance seems to drop a bit in both FakeIDet and FakeIDet2.

These results prove the technical contributions of FakeIDet2 over FakeIDet [25], i.e., Patch Embedding Extractor and the Patch Embedding Fusion, that not only allows detecting attacks where the entire ID is a fake (i.e., print or screen), but also attacks where small sections are fake (i.e., composite). Given that the performance using the 64×64 patch size configuration is close to the 128×128 patch size, we selected this patch size for further experiments, as it increases privacy in real-world settings, which is the main purpose of the study.

### 6.3. Anonymization vs. Performance

In this section, we analyze the impact on performance when removing sensitive information from an ID. To do so, we train FakeIDet2 in the 64×64 patch size configuration at all anonymization levels, and evaluate the performance using Non-Anonymized data. This scenario simulates realistic real-world settings in which ID Holders have some restrictions when sharing IDs to AI Researchers in order to train the fake ID detectors. Table 6 shows the performance of FakeIDet2 in terms of EER (%) for the different anonymization levels and attacks. A particular trend can be observed: the fake ID detection errors (per attack and overall) increase as we reduce the amount of sensitive information, which shows that FakeIDet2 performance depends on the amount of sensitive information available in the training stage (3.99% in Non-Anonymized vs. 8.64% in Pseudo-Anonymized vs. 17.94% in Fully-Anonymized). Even with this drop in terms of performance, we observe that the Pseudo-Anonymized 64×64 configuration performs fairly well despite having seen only partial information of the ID, which supports our proposed hypothesis that training a model not using all the sensitive information of the ID may generate a small loss in performance as a trade-off. Given that this preliminary analysis confirmed that training with Pseudo-Anonymized data using 64×64 patch size remains competitive, we de-

Model	Screen	Print	Composite	All
Non-Anonymized	<b>4.53</b>	<b>1.45</b>	<b>7.17</b>	<b>3.99</b>
Pseudo-Anonymized	5.01	4.89	16.29	8.64
Fully-Anonymized	8.98	5.77	26.54	17.94

Table 6: Performance of FakeIDet2 in terms of EER (%) when training over the different anonymization levels for the  $64 \times 64$  patch size configuration. Results are achieved using the final evaluation of FakeIDet2-db, considering Non-Anonymized IDs.

Training	Screen	Print	Composite	All
No-Screen	36.00	1.00	7.17	19.93
No-Print	3.05	6.77	12.25	7.97
No-Composite	2.02	0.00	50.96	28.24
All-Attacks	5.01	4.89	16.29	8.64

Table 7: Performance of FakeIDet2 in terms of EER (%) for the leave-one-attack-out scenario, i.e., leaving one of the PAIs out from the training dataset. These results are obtained evaluating with all PAIs, including the one left out in each case.

cided to use this configuration for the rest of our experiments, as it is balanced in terms of privacy and performance, which is the purpose of the study.

#### 6.4. Leave-One-Attack-Out Scenario

Table 7 provides the results of FakeIDet2 when different attacks are left out of the training data. For reference, we include EER for FakeIDet2 when trained using all PAIs available (All-Attacks). Based on our previous findings, we consider for training FakeIDet2 the Pseudo-Anonymized  $64 \times 64$  patch configuration, due to privacy reasons. The final evaluation is carried using Non-Anonymized  $64 \times 64$  patch configuration.

The worst results in terms of EER are obtained when composite attacks are left out, with a 28.24% when evaluating all types of attacks. This shows that the physical composite attacks included in our new FakeIDet2-db are the harder attacks for our model to detect, with 50.96% EER. It is also interesting to note that our screen attacks seem difficult to detect when they are out of training, with 36.00% EER. Finally, in the case of the print attacks, FakeIDet2 performs much better compared to detecting the other attacks with just a 6.77% in terms of EER when only detecting print attacks, although a little caveat should be considered. As covered in Sec. 3, our physical composite attacks are created by using small crops from print attacks and lying them over real IDs. We argue that FakeIDet2 may be leveraging those learned features from composite patches to predict print attacks appropriately, giving competitive results that even improve the performance when the whole dataset is available (8.64% EER vs 7.97% EER).

Finally, an interesting phenomenon is observed when training FakeIDet2 leaving one attack out: the fake detector seems to “specialize” in detecting the attacks that are used in training, since the EER becomes even lower compared to the case of training using all attacks. For example, when leaving the composite attacks, FakeIDet2 obtains an EER of 2.02% when detecting print attacks,



Model	Screen	Print	Composite	All
No-iPhone	22.12	30.98	30.63	22.61
No-Xiaomi	3.96	1.94	14.24	8.30
No-Redmi	8.07	1.94	7.13	8.97
All-Devices	5.01	4.89	16.29	8.64

Table 8: Performance of FakeIDet2 in terms of EER (%) for the leave-one-sensor-out scenario, i.e., leaving one of the acquisition devices out from the training dataset. These results are obtained evaluating with data from all the acquisition devices in the Non-Anonymized,  $64 \times 64$  patch configuration including the one left out in each case.

compared to 5.01% which is obtained when trained with all attacks. This can be expected, as when the number of classes is smaller, the data distribution to model by FakeIDet2 becomes simpler, hence becoming better at detecting the only attacks presented at training time.

#### 6.5. Leave-One-Sensor-Out Scenario

Table 8 provides the results of FakeIDet2 when different acquisition sensors are left out of the training data. For reference, we include EER for FakeIDet2 when trained using all available devices (All-Devices). Based on our previous findings, we consider for training FakeIDet2 the Pseudo-Anonymized  $64 \times 64$  patch configuration, due to privacy reasons. The final evaluation is carried using Non-Anonymized  $64 \times 64$  patch configuration.

As can be seen in the table, performance decreases when the highest quality sensor (i.e., iPhone 15) is not used in training but only in the final evaluation. This seems not to be happening in the rest of the scenarios, where images from the iPhone 15 are present in the training set. Given the different experiments that we run regarding this issue, our intuition on why this is happening relies on the fact that iPhone 15 cameras capture finer details that give more distinct features compared to Xiaomi’s and Redmi’s sensors. These fine-grain characteristics allow our FakeIDet2 to focus on traces that are more subtle, such as Moiré patterns on the screen attacks and the droplets of ink from the print and composite attacks, given that these attacks were printed with an Inkjet-kind printer. Furthermore, one of the main features of the AdaFace loss function is that the adaptive margins change depending on the image quality. When using images of high quality along with images of low or medium quality, the database is more diverse, and AdaFace helps the learning process by establishing larger margins for high quality images and lower for low quality images. If images of low quality are the majority of the database, the margins may not be as large as desired for proper separation between classes, and the features per each class may be overlapped in the embedded space, which are not helpful when forwarded into the Patch Embedding Fusion module, harming the performance.

#### 6.6. Cross-Database Scenario

This section evaluates the performance of FakeIDet2 trained through the selected configuration (i.e., Pseudo-Anonymized  $64 \times 64$  patch size) on different public databases in the literature. Concretely, we consider DLC-2021 [30], KID34K [28] and Benalcazar *et al.* synthetic database from [5]. For this evaluation, we sample around 10,000 images from KID34K, balancing between PAIs

PAI	DLC-2021 [30]	KID34K [28]	Benalcazar <i>et al.</i> [5]
Screen	5.02	13.41	N/A
HQ-Print	10.28	18.26	N/A
Print	12.45	4.99	N/A
Gray-Print	10.60	N/A	N/A
Synthetic	N/A	N/A	39.41
<b>All</b>	<b>8.90</b>	<b>13.84</b>	<b>39.41</b>

Table 9: Performance of FakeIDet2 in terms of EER (%) per type of attack and database. In order to facilitate the collaboration between ID Holders and AI Researchers, we consider the privacy-aware scenario where FakeIDet2 is trained using the Pseudo-Anonymized  $64 \times 64$  patch size configuration.

and ID owners, and approximately 30,000 images from several DLC-2021 videos, sampling in a similar way as in KID34K. DLC-2021 contains Spanish IDs, but they are from the first version, which are not seen during training FakeIDet2 as described in Sec. 5.1. Regarding the real IDs, as in those databases the “real” IDs were created by the researchers under laboratory conditions, that is, they are not official IDs, we consider the aforementioned databases as attacks. Real IDs are extracted from the evaluation dataset of our FakeIDet2-db, similar to previous experiments, since they are official IDs. Our aim with this privacy-aware scenario is to assess the generalization ability of our proposed FakeIDet2 to unseen conditions, e.g., different PAIs, templates, devices, etc.

Table 9 shows the performance of FakeIDet2 in terms of EER (%) per type of attack and database. In order to facilitate the collaboration between ID Holders and AI Researchers, we consider the privacy-aware scenario where FakeIDet2 is trained using the Pseudo-Anonymized  $64 \times 64$  patch size configuration. For DLC-2021 and KID34K we denote by “HQ-Print” the types of print attacks which are proposed as “real” in each of the databases, and for Benalcazar *et al.* we denote “Synthetic” the samples that have been created via generative methods trained from real samples. Furthermore, in case a database does not contain a specific attack, it is denoted as “N/A”.

As can be seen in Table 9, the performance per PAI varies between databases. For example, FakeIDet2 is worse in screen attacks from the KID34K database compared to the DLC-2021, with 13.41% vs. 5.02% EER, respectively. This could be motivated by the amount of devices that were used to create screen attacks in KID34K, ranging from smartphones, tablets, laptops, and LCD monitors. A similar trend can be observed for the HQ-Print attacks, where the KID34K samples seem to confuse FakeIDet2 more (18.26% vs 10.28% EER). This may be induced by the variability in terms of acquisition devices (12 in KID34K vs. 2 in DLC-2021), with different specifications that create different traces or fingerprints in the images taken. Regarding print attacks, we see that our model performs better on the KID34K dataset than in DLC-2021 (4.99% vs. 12.45%). This might be produced because KID34K follows a similar approach to ours, i.e., print attacks are created after printed and then laminated. Finally, for the synthetic attacks included in Benalcazar *et al.* database, FakeIDet2 is not able to generalize well to this unseen attack (39.41% EER). This result is expected due to the following reasons: *i*) the data (both real and fake

ID samples) used to train FakeIDet2 are only based on physical acquisitions using smartphone cameras, not synthetic data, and *ii*) according to [5], those synthetic samples were generated using GANs trained with official Chilean ID samples, which means that they share similar characteristics with real IDs that may confuse FakeIDet2.

In conclusion, our proposed privacy-aware scenario in order to promote the collaboration between ID Holders and AI Researchers has provided very interesting results, despite the fact that our proposed FakeIDet2 is only trained through the Pseudo-Anonymized  $64 \times 64$  patch size configuration, using the development set of FakeIDet2-db. Under unseen physical attacks, FakeIDet2 is able to achieve 8.90% EER on DLC-2021 and 13.84% on KID34K, as can be seen in Table 9. We expect that these results can be enhanced in real-world settings, as the ID Holders own large-scale ID databases that can be exploited to improve the machine learning processes described here.

## 7. Conclusion

In this article, we have explored a novel framework for privacy-aware fake ID detection, which bridges the existing gap between IDs Holders (e.g., governments, police, banks, etc.), which provide digital services to citizens and own large-scale datasets of real IDs, and AI Researchers, which have the experience and technology to develop fake ID detectors, but not the data.

In order to advance in the field, we have first introduced FakeIDet2-db, a database that complies with the proposed framework, which contains more than 900K patches in different sizes ( $128 \times 128$  and  $64 \times 64$ ), extracted from a total of 2,000 images of pseudo-anonymized and fully-anonymized IDs. Regarding real and fake IDs, to our knowledge, this is the first database that contains: *i*) official real IDs captured under several conditions regarding camera sensor, illumination conditions and distance, and *ii*) physical composite attacks. In addition, our database considers a large variability during the acquisition, e.g., using three different smartphones, and changes in illumination and height conditions.

Together with FakeIDet2-db, we have presented FakeIDet2, a new method for the detection of fake ID that is sensitive to privacy and utilizes patches from IDs and varying levels of anonymization to protect sensitive information. We show that learning embeddings from patches extracted from real and fake IDs is a crucial step for effective fake ID detection. Considering the nature of the problem, especially for physical composite attacks, we have proposed a method that explicitly accounts for class imbalance using time-adaptive class weights [14] during learning and have compared it to other popular loss functions [23], achieving superior performance compared to traditional approaches (CosFace, ArcFace, and AdaFace). Using patch-level embeddings, we have incorporated a learnable fusion module based on multi-head self-attention [4] to assign different weights to different patches within a single ID, producing an ID-level prediction that indicates whether the submitted ID is real or fake. Furthermore, we have evaluated the impact of different anonymization levels and patch sizes, showing that our FakeIDet2 remains competitive in privacy-aware scenarios, as compared to fully visible data settings (3.99% in non-anonymized vs. 8.64% in pseudo-anonymized).

Finally, we have also introduced an extensive and reproducible public benchmark, which considers, in addition to our FakeIDet2-db, other public databases

in the literature, containing unseen physical (KID34K [28], DLC-2021 [30]) and synthetic attacks (Benalcazar *et al.* [5]) to assess performance in different data distributions that contain IDs from several demographic regions (i.e., Europe, Asia, and South America).

The results achieved by FakeIDet2 (Pseudo-Anonymized  $64 \times 64$  patch size configuration) in the proposed benchmark under unseen conditions, 8.90% EER on DLC-2021 and 13.84% on KID34K, promote our proposed privacy-aware scenario in order to facilitate the collaboration between ID Holders and AI Researchers in real-world settings.

In future work, we will explore other foundation models [27] and other learning architectures based on the patch-based principles shown in Fig. 6 and other non-patch and inpainting detection methods [8] following ongoing benchmarks and competitions such as DeepID<sup>10</sup>. Improving the accuracy of FakeIDet2 by exploiting the spatial context of patches (e.g., using spatial attention [10] and local quality measures [31]) and a full layout analysis [19] is also in our plans.

## Acknowledgements

Funding from INTER-ACTION (PID2021-126521OBI00 MICINN/FEDER), M2RAI (PID2024-160053OB-I00 MICIU/FEDER), Cátedra ENIA UAM-Veridas en IA Responsable (NextGenerationEU PRTR TSI-100927-2023-2), and PowerAI+ (SI4/PJI/2024-00062 Comunidad de Madrid and UAM).

## References

- [1] Arlazarov, V.V., Bulatov, K., Chernov, T., Arlazarov, V.L., 2019. MIDV-500: A Dataset for Identity Document Analysis and Recognition on Mobile Devices in Video Stream. *Computer Optics* 43.
- [2] Aslett, K., Sanderson, Z., Godel, W., Persily, N., Nagler, J., Tucker, J.A., 2024. Online Searches to Evaluate Misinformation Can Increase Its Perceived Veracity. *Nature* 625, 548–556.
- [3] Ba, J.L., Kiros, J.R., Hinton, G.E., 2016. Layer Normalization. *arXiv preprint arXiv:1607.06450* URL: <https://arxiv.org/abs/1607.06450>, *arXiv:1607.06450*.
- [4] Bahdanau, D., Cho, K., Bengio, Y., 2016. Neural Machine Translation by Jointly Learning to Align and Translate. URL: <https://arxiv.org/abs/1409.0473>, *arXiv:1409.0473*.
- [5] Benalcazar, D., Tapia, J.E., Gonzalez, S., Busch, C., 2023. Synthetic ID Card Image Generation for Improving Presentation Attack Detection. *IEEE Transactions on Information Forensics and Security* 18, 1814–1824.
- [6] Bulatov, K., Emelianova, E., Tropin, D., et al., 2022. MIDV-2020: A Comprehensive Benchmark Dataset for Identity Document Analysis. *Computer Optics* 46.

---

<sup>10</sup><https://deepid-iccv.github.io/>

- [7] Bulatov, K., Matalov, D., Arlazarov, V.V., 2020. MIDV-2019: Challenges of the Modern Mobile-Based Document OCR, in: Proceedings of the International Conference on Machine Vision, pp. 818–824.
- [8] Daryani, A.E., Mirmahdi, M., Hassanpour, A., Shahreza, H.O., Yang, B., Fierrez, J., 2023. IRL-Net: Inpainted region localization network via spatial attention. *IEEE Access* 11, 115677–115687.
- [9] DeAlcala, D., Morales, A., Fierrez, J., Mancera, G., Tolosana, R., Ortega-Garcia, J., 2025a. Active membership inference test (aMINT): Enhancing model auditability with multi-task learning, in: IEEE/CVF International Conference on Computer Vision.
- [10] DeAlcala, D., Morales, A., Fierrez, J., Tolosana, R., 2025b. AttZoom: Attention zoom for better visual features, in: Proceedings IEEE/CVF Intl. Conf. on Computer Vision Workshops. URL: <https://arxiv.org/abs/2508.03625>.
- [11] Deng, J., Guo, J., Xue, N., Zafeiriou, S., 2019. ArcFace: Additive Angular Margin Loss for Deep Face Recognition, in: Proceedings of the IEEE/CVF Conference on Computer Vision and Pattern Recognition, pp. 4690–4699.
- [12] Fang, M., Huber, M., Fierrez, J., et al., 2023. SynFacePAD 2023: Competition on Face Presentation Attack Detection Based on Privacy-aware Synthetic Training Data, in: Proceedings IEEE/IAPR International Joint Conference on Biometrics, pp. 1–11.
- [13] Feng, S., Tramèr, F., 2024. Privacy Backdoors: Stealing Data with Corrupted Pretrained Models, in: Proceedings of the 41st International Conference on Machine Learning, pp. 13326–13364.
- [14] Fierrez, J., Morales, A., Vera-Rodriguez, R., Camacho, D., 2018. Multiple classifiers in biometrics. Part 2: Trends and challenges. *Information Fusion* 44, 103–112.
- [15] Gonzalez, S., Tapia, J.E., 2025. Forged Presentation Attack Detection for ID Cards on Remote Verification Systems. *Pattern Recognition* 162, 111352.
- [16] Hernandez-Ortega, J., Fierrez, J., Morales, A., Galbally, J., 2023. Introduction to Presentation Attack Detection in Face Biometrics and Recent Advances, in: S. Marcel, J. Fierrez, N.E. (Ed.), *Handbook of Biometric Anti-Spoofing*, Springer. pp. 203–230. 3rd Ed.
- [17] Kim, M., Jain, A.K., Liu, X., 2022. AdaFace: Quality adaptive margin for face recognition, in: Proceedings of the IEEE/CVF Conference on Computer Vision and Pattern Recognition, pp. 18750–18759.
- [18] Liu, H., Wang, W., Sun, H., Rocha, A., Li, H., 2024. Robust Domain Misinformation Detection via Multi-Modal Feature Alignment. *IEEE Transactions on Information Forensics and Security* 19, 793–806.

- [19] Lopez-Duran, M., Fierrez, J., Morales, A., et al., 2025. Benchmarking graph neural networks for document layout analysis in public affairs, in: Proc. Intl. Conf. on Document and Analysis Workshops (ICDARw). URL: <https://arxiv.org/abs/2505.14699>.
- [20] Markham, R.P., López, J.M.E., Nieto-Hidalgo, M., Tapia, J.E., 2024. Open-Set: ID Card Presentation Attack Detection Using Neural Style Transfer. *IEEE Access* 12, 68573–68585.
- [21] Melzi, P., Rathgeb, C., Tolosana, R., Vera-Rodriguez, R., Lawatsch, D., Domin, F., Schaubert, M., 2023. GANDiffFace: Controllable Generation of Synthetic Datasets for Face Recognition with Realistic Variations, in: Proceedings of the IEEE/CVF International Conference on Computer Vision Workshops, pp. 3086–3095.
- [22] Melzi, P., Tolosana, R., Vera-Rodriguez, R., Kim, M., Rathgeb, C., Liu, X., DeAndres-Tame, I., Morales, A., Fierrez, J., Ortega-Garcia, J., et al., 2024. FRCSyn-onGoing: Benchmarking and Comprehensive Evaluation of Real and Synthetic Data to Improve Face Recognition Systems. *Information Fusion* 107, 102322.
- [23] Morales, A., Fierrez, J., Acien, A., Tolosana, R., Serna, I., 2022. SetMargin Loss applied to deep keystroke biometrics with circle packing interpretation. *Pattern Recognition* 122, 108283.
- [24] Mudgalgundurao, R., Schuch, P., Raja, K., Ramachandra, R., Damer, N., 2022. Pixel-Wise Supervision for Presentation Attack Detection on Identity Document Cards. *IET Biometrics* 11, 383–395.
- [25] Muñoz-Haro, J., Tolosana, R., Vera-Rodriguez, R., Morales, A., Fierrez, J., 2025. FakeIDet: Exploring Patches for Privacy-Preserving Fake ID Detection, in: Proceedings IEEE/IAPR International Joint Conference on Biometrics. URL: <https://arxiv.org/abs/2504.07761>.
- [26] Neves, J.C., Tolosana, R., Vera-Rodriguez, R., Lopes, V., Proenca, H., Fierrez, J., 2020. GANprintR: Improved fakes and evaluation of the state of the art in face manipulation detection. *IEEE Journal of Selected Topics in Signal Processing* 14, 1038–1048.
- [27] Oquab, M., Darcet, T., Moutakanni, T., Vo, H.V., Szafraniec, M., Khali-dov, V., Fernandez, P., HAZIZA, D., Massa, F., El-Nouby, A., Assran, M., Ballas, N., Galuba, W., Howes, R., Huang, P.Y., Li, S.W., Misra, I., Rabbat, M., Sharma, V., Synnaeve, G., Xu, H., Jegou, H., Mairal, J., Labatut, P., Joulin, A., Bojanowski, P., 2024. DINOv2: Learning Robust Visual Features Without Supervision. *Transactions on Machine Learning Research* .
- [28] Park, E.J., Back, S.Y., Kim, J., Woo, S.S., 2023. KID34K: A Dataset for Online Identity Card Fraud Detection, in: Proc. of the 32nd ACM Intl. Conf. on Information and Knowledge Management, pp. 5381–5385.
- [29] Peña, A., Fierrez, J., Morales, A., Mancera, G., Lopez, M., Tolosana, R., 2025. Addressing Bias in LLMs: Strategies and Application to Fair AI-based Recruitment, in: Proceedings AAAI/ACM Conference on AI, Ethics, and Society. URL: <https://arxiv.org/abs/2506.11880>.

- [30] Polevoy, D.V., Sigareva, I.V., Ershova, D.M., et al., 2022. Document Liveness Challenge Dataset (DLC-2021). *Journal of Imaging* 8.
- [31] Schlett, T., Rathgeb, C., Henniger, O., Galbally, J., Fierrez, J., Busch, C., 2022. Face image quality assessment: A literature survey. *ACM Computing Surveys* 10, 1–49.
- [32] Shahreza, H.O., Ecabert, C., George, A., Unnervik, A., Marcel, S., et al., 2024. SDFR: Synthetic Data for Face Recognition Competition, in: *Proceedings 18th International Conference on Automatic Face and Gesture Recognition*, pp. 1–9.
- [33] Soares, A., Batista, R., Leite, B., 2020. BID Dataset: a Challenge Dataset for Document Processing Tasks, in: *Anais Estendidos da Conference on Graphics, Patterns and Images*, pp. 143–146.
- [34] Tapia, J.E., Damer, N., Busch, C., et al., 2024. First Competition on Presentation Attack Detection on ID Card, in: *Proceedings of the IEEE International Joint Conference on Biometrics*, pp. 1–10.
- [35] Tolosana, R., Romero-Tapiador, S., Vera-Rodriguez, R., Gonzalez-Sosa, E., Fierrez, J., 2022a. Deepfakes detection across generations: Analysis of facial regions, fusion, and performance evaluation. *Engineering Applications of Artificial Intelligence* 110, 104673.
- [36] Tolosana, R., Vera-Rodriguez, R., Fierrez, J., Morales, A., Ortega-Garcia, J., 2022b. *Handbook of Digital Face Manipulation and Detection*. Springer. chapter An Introduction to Digital Face Manipulation. pp. 3–26.
- [37] Verdoliva, L., 2020. Media Forensics and DeepFakes: An Overview. *IEEE Journal of Selected Topics in Signal Processing* 14, 910–932.
- [38] Wang, H., Wang, Y., Zhou, Z., Ji, X., Gong, D., Zhou, J., Li, Z., Liu, W., 2018. CosFace: Large margin cosine loss for deep face recognition, in: *Proceedings of the IEEE/CVF Conference on Computer Vision and Pattern Recognition*, pp. 5265–5274.
- [39] Xie, L., Wang, Y., Guan, H., Nag, S., Goel, R., Swamy, N., Yang, Y., Xiao, C., Prisby, J., Maciejewski, R., Zou, J., 2024. IDNet: A Novel Identity Document Dataset via Few-Shot and Quality-Driven Synthetic Data Generation, in: *Proceedings of the IEEE International Conference on Big Data*, pp. 2244–2253.
- [40] Zhang, Y., Jia, R., Pei, H., Wang, W., Li, B., Song, D., 2020. The Secret Revealer: Generative Model-Inversion Attacks Against Deep Neural Networks, in: *Proceedings of the IEEE/CVF Conference on Computer Vision and Pattern Recognition*, pp. 250–258.